Combined Fluorescence and NMR Studies of Reversed HPLC Stationary Phases with Different Ligand Chain Lengths

H.-J. Egelhaaf,[1,3] D. Oelkrug,[1] M. Pursch,[2] and K. Albert[2]

Alkyl chain bonded "reversed" HPLC phases consisting of 6 to 30 carbon atoms are investigated by fluorescence spectroscopy, steady-state and time-resolved fluorescence anisotropy, and solid-state NMR spectroscopy. The structure and dynamics of the interphase formed by alkyl chains and liquid phase penetrating each other are studied as a function of alkyl chain length. Increasing alkyl chain lengths lead to enhanced partitioning of the fluorescent probe diphenylhexatriene (DPH) into the interphase, as monitored by fluorescence decay curves. The concomitant spectral red shift of DPH fluorescence excitation maxima is evidence of increased interphase polarizability. Time-resolved fluorescence anisotropy measurements reveal that the motion of the probe molecule in the interphase is "wobble in cone"-like. Cone angles θ and rotational correlation times τ_R change from $\theta = 63°$ and $\tau_R = 0.75$ ns in C_6 phases to $\theta = 42°$ and $\tau_R = 1.50$ ns in C_{30} phases, thus indicating decreasing probe mobility with increasing ligand length. This interpretation is supported by ^{13}C CP/MAS NMR spectra, which show reduced contributions of alkyl chain gauche conformations, i.e., enhanced interphase order, in phases with long alkyl chains and high surface coverage. A concomitant increase in the line-widths of ^1H MAS NMR peaks indicates reduced mobility of the longer chains. The spectroscopic observations are consistent with the results of HPLC separations, where enhanced shape selectivity is found with increasing ligand length, rod-shaped molecules like DPH showing the greatest increase in retention time.

KEY WORDS: HPLC stationary phases; ligand length; solid-state NMR spectroscopy; time resolved fluorescence anisotropy.

INTRODUCTION

Octadecyl (C_{18}) bonded silica gel is the standard material in HPLC for the separation of polycyclic aromatic hydrocarbons (PAHs). Since it has been realized that selectivity increases with alkyl phase length,[1-5] also phases with longer ligands, up to C_{30} and C_{34}, have be-

come popular. In terms of the "slot" model, deeper slots are responsible for the enhanced shape selectivity of longer alkyl chain phases.[5] However, also negative effects, e.g., reduced mass transfer rates, are observed with increasing thickness of the bonded phase.[5] Optimization of chromatographic materials thus requires an understanding of the influence of ligand chain length on the structure and dynamics of the bonded phase on a molecular level.

A variety of chromatographic and spectroscopic methods has been applied to study the effect of ligand chain length on selectivity. Solid-state NMR investigations have shown that the conformational order and mo-

[1] Institute for Physical and Theoretical Chemistry, University of Tübingen, Auf der Morgenstelle 8, 72076 Tübingen, Germany.
[2] Institute for Organic Chemistry, University of Tübingen, Auf der Morgenstelle 18, 72076 Tübingen, Germany.
[3] To whom correspondence should be addressed. Fax: +49 7071/296910. e-mail: hans-joachim.egelhaaf@uni-tuebingen.de.

bility of bonded alkyl phases is strongly chain length dependent.[6,7] Fluorescence quenching experiments have shown that protection of the sorbed fluorescence probe from the quencher increases with alkyl chain length.[8] Pyrene excimer formation has been used to determine the microviscosity in C_2, C_8, and C_{18} layers.[9] Chain-length dependent microviscosities have also been found by time-resolved fluorescence anisotropy measurements on alkyl bonded planar silica surfaces, using the TIRF technique.[10] This method has also been applied to investigate the orientation of the solute in the bonded phase.[11] However, caution should be used in extrapolating results obtained from TIRF studies on planar surfaces to porous particles, as the former show a higher degree of chain ordering and hence less absorption of mobile phase.[12]

In this work, the selectivity, structure and dynamics of alkyl chain bonded chromatographic phases with 6 to 30 carbon atoms (Fig. 1) are studied as a function of alkyl chain length. Solid-state NMR spectroscopy is used to determine the conformation and mobility of the bonded phase. A well characterized fluorescent probe,[13] diphenylhexatriene (DPH), is added to the liquid phase, in order to study the effect of ligand chain length on solute–alkyl phase interaction. Steady-state and time-resolved fluorescence anisotropy measurements are employed to investigate the mobility of DPH sorbed in the bonded phase. Fluorescence spectra and fluorescence lifetime measurements serve to determine the fraction of solute partitioning into the alkyl phase. The spectroscopic data are compared to the results of HPLC separations.

EXPERIMENTAL

Materials

C_6, C_{18}, and C_{30} monomeric phases on Lichrospher (Si 100, 5-μm silica; Merck, Darmstadt, Germany) were synthesized according to procedures described previously.[14,15]

The ligand density of all three phases was in the range of 4.0–4.7 μmol · m^{-2}.

Fluorescence and Absorption Measurements

All fluorescence measurements were carried out on suspensions, which were prepared by adding 4 mg of reversed phase to 10^{-7} M solutions of DPH in 3.0 ml of acetonitrile (UVASOL, Merck)/water mixture (1:2, v/v).

At this silica concentration no fluorescence depolarization by multiple scattering was observed. The suspensions were agitated with a magnetic stirrer to prevent sedimentation. Steady-state fluorescence spectra and fluorescence anisotropy spectra were recorded on a SPEX 222 fluorometer equipped with Glan-Thompson polarizers.

Fluorescence decay curves were obtained on a SPEX 112 fluorometer applying the single-photon counting technique. A thyratron-controlled nanosecond flashlamp was used as light source. Time-resolved anisotropy decay curves were obtained at the Center for Fluorescence Spectroscopy in Baltimore, MD, by single-photon counting. As excitation source a cavity-dumped, frequency-doubled pyridine 1 laser was used (λ_{ex} = 360 nm, fwhm = 7 ps). A microchannel plate photomultiplier (Hamamatsu R2809) provided an instrument response of approximately 60 ps.

Fluorescence lifetimes were obtained from a single or double exponential analysis of the fluorescence decay curves, $I_F(t)$,

$$I_F(t) = \sum_i A_i \exp(-t/\tau_{F,i}) \tag{1}$$

where $\tau_{F,i}$ represents the decay time of the ith component and A_i its amplitude.

Anisotropy decay curves $r(t)$ were obtained from

$$r(t) = D(t)/S(t) \tag{2}$$

where $D(t) = I_{vv}(t) - g \cdot I_{vh}(t)$ and $S(t) = I_{vv}(t) + 2g \cdot I_{vh}(t)$. The scaling factor $g = I_{hv}/I_{hh}$ was determined for each experiment. I_{vv}, I_{vh}, I_{hv}, and I_{hh} stand for the observed fluorescence intensities, where the first and second indices indicate the positions (v = vertical, h = horizontal) of polarizer and analyzer, respectively.

In the case of a single fluorescing species, the decay of the fluorescence anisotropy, $r(t)$, after a short laser pulse is exponential,[16]

$$r(t) = (r_0 - r_\infty) \cdot e^{-(t/\tau_R)} + r_\infty \tag{3}$$

where r_0 is the anisotropy at $t = 0$, τ_R is the rotation correlation time, and r_∞ is the residual anisotropy for $t \to \infty$. For unrestricted motion, $r_\infty = 0$. If the diffusional motion of the fluorophore is restricted to a solid cone ("wobble-in-cone"; see Fig. 1),

$$\frac{r_\infty}{r_0} = [0.5 \cdot \cos\theta(\cos\theta + 1)]^2 \tag{4}$$

where θ is the half-cone angle as defined in Fig. 1.

If several fluorescing species, i, are present, with different rotation correlation times, $\tau_{R,i}$, and different flu-
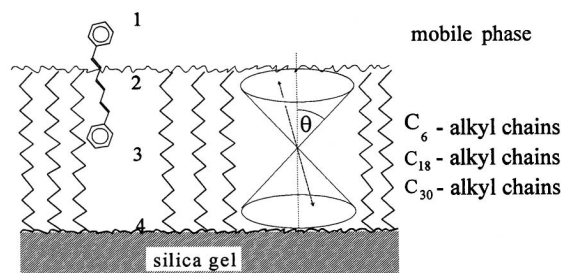
Fig. 1. Schematic representation of the studied systems. C_6, C_{18}, and C_{30} denote silica bonded hexyl, octadecyl, and triacontyl chains, respectively. For the sake of clarity, alkyl chains are shown as fully extended. The mobile phase is an acetonitrile/water mixture (2:1, v/v). The probe molecule, diphenylhexatriene (DPH), performs a wobble-like motion in a cone defined by the half-cone angle θ, which is determined by the size of the interstices between the alkyl phases.

Table I. Fluorescence Lifetimes, τ_F, and Quantum Yields, Φ_F, of DPH in Different Deaerated Solvents

Solvent	τ_F (ns)	Φ_F
n-Hexane[a]	15.9	0.62
n-Decane[a]	14.0	0.68
Ethanol[a]	5.6	0.26
Acetonitrile[a]	4.1	0.17
Acetonitrile/water (1:2)	1.2	0.04

[a] From Ref. 17.

orescence lifetimes, $\tau_{F,i}$, the decay is described by Eq. (5):

$$r(t) = \frac{\sum_i I_{F,i}(t) \cdot r_i(t)}{\sum_i I_{F,i}(t)} = \frac{\sum_i A_i \cdot e^{-(t/\tau_{F,i})} \cdot [(r_{0,i} - r_{\infty,i}) \cdot e^{-(t/\tau_{R,i})} + r_{\infty,i}]}{\sum_i A_i \cdot e^{-(t/\tau_{F,i})}} \quad (5)$$

Solid-State NMR Measurements

^{13}C and ^{1}H solid-state NMR spectra were obtained on a Bruker ASX 300 NMR spectrometer at 7.1 T. For ^{1}H-MAS-NMR measurements the samples were packed into double-bearing 4-mm rotors, which were spun at 14 kHz by dry air gas drive; the recycle delay was 4 s and the 90° pulse length was 4.4 μs. ^{13}C-CP/MAS-NMR measurements were carried out with 7-mm rotors (proton 90° pulse length: 4.4 μs). The contact time was 6 ms,

Table II. Fluorescence Lifetimes, τ_F, and Amplitudes, A, Obtained from a Biexponential Analysis of the Fluorescence Decay Traces Observed for DPH in Suspensions of C_6, C_{18}, and C_{30} HPLC Phases in Acetonitrile/Water Mixtures[a]

Phase	τ_F (ns)	A	x	α
C_6				
Stationary	3.4	0.24	0.19	110
Mobile	0.7	0.76	0.81	
C_{18}				
Stationary	6.1	0.52	0.53	510
Mobile	0.9	0.48	0.47	
C_{30}				
Stationary	6.4	0.56	0.56	570
Mobile	1.0	0.44	0.44	

[a] Stationary: DPH sorbed in the alkyl phase. Mobile: DPH dissolved in the mobile phase. x is the molar fraction of DPH in the respective phase. $\alpha = c_{stat}/c_{mob}$ is the corresponding partition coefficient between the stationary and the mobile phase, inserting $\rho = 0.6$ g · cm^{-3} for the skeletal density of silica gel.

the recycle delay was 1 s, and the spinning speed was 4.0 kHz.

RESULTS AND DISCUSSION

DPH was chosen as fluorescent probe because it combines several useful properties. It is a well-characterized probe for fluorescence anisotropy investigations in lipophilic media, mostly in the determination of microviscosities of biological membranes.[16] Also, the photophysical properties of DPH are strongly dependent on its local environment,[17] which enables us to distinguish between DPH dissolved in the mobile phase and DPH sorbed in the alkyl phase, respectively. The absorption spectrum undergoes a red shift with increasing polarizability of the environment. Radiative decay rates rise with increasing solvent polarizability and nonradiative decay rates grow with increasing solvent polarity.[17] Thus fluorescence lifetimes and quantum yields in acetonitrile and in acetonitrile/water mixtures are considerably lower than in alcohols or in alkanes, as illustrated by the data given in Table I for DPH in different solutions.

Fluorescence decay curves of DPH in suspensions of the HPLC phases in acetonitrile/water mixtures can be fitted with two exponentials (Table II). The shorter-lived component has a lifetime of $\tau_F \approx 1$ ns, which is close to the value observed in acetonitrile/water mixtures and is, therefore, assigned to molecules solvated by the mobile phase. The longer-lived component varies from
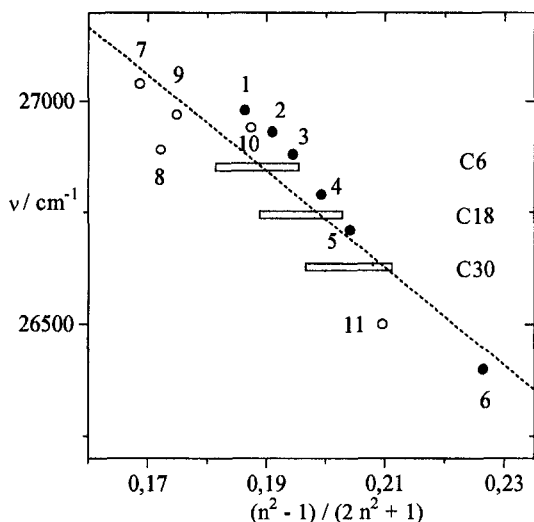
Fig. 2. Spectral positions of the absorption maxima of DPH vs the polarizability of its microenvironment, given by the Onsager function. Circles: DPH in bulk solutions. Filled circles represent hydrocarbons (1, hexane; 2, heptane; 3, octane; 4, decane; 5, cyclohexane; 6, toluene). Open circles represent nonhydrocarbons (1, methanol; 2, acetonitrile; 3, acetonitrile/water; 4, ethanol; 5, isopropanol; 6, chloroform). The dashed line is a linear regression to all data points obtained in solution. Bars represent the absorption maxima found for DPH in suspensions of C_6, C_{18}, and C_{30} phases in acetonitrile/water mixtures (1: 2, v/v). The width of the bars corresponds to the uncertainty of the corresponding interphase polarizabilities.
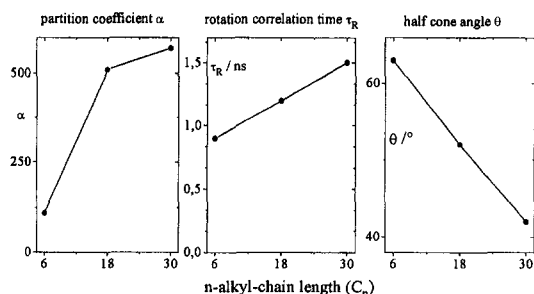

Fig. 3. Properties of the probe molecule, DPH, as a function of ligand chain length. Left: Partition coefficient $\alpha = c_{stat}/c_{mob}$, where c_{stat} and c_{mob} are the concentrations of DPH in the stationary and mobile phase, respectively. Middle: Rotation correlation time, τ_R, of DPH sorbed in the interphase. Right: Residual anisotropy, r_∞, of DPH sorbed in the interphase.

$\tau_F = 3.4$ ns for C_6 to $\tau_F = 6.4$ ns for C_{30}. In C_{30} phases no oxygen quenching effect on the long component lifetime was measurable at atmospheric oxygen partial pressure. These lifetimes are considerably longer than the lifetime of DPH in the mobile phase and are therefore ascribed to molecules which are totally or partially immersed in the interphase formed by the alkyl chains and

the wetting component of the solvent mixture, i.e., acetonitrile. With no reliable fluorescence quantum yields at hand, it cannot be decided unambiguously whether the increase in the fluorescence lifetime of DPH upon its sorption in the interphase is caused mainly by polarity or polarizability effects. However, it seems a sound assumption that the fluorescence lifetimes are affected by both the polarity and the polarizability of the alkyl phase. On one hand, it has long been known that the polarity of the interphase changes with the alkyl chain length,[12,18] being close to that of bulk 1-octanol in the case of C_{18} phases.[19] On the other hand, the spectral red shift of the fluorescence excitation spectra of DPH with increasing chain length shows that the polarizability also increases (Fig. 2). At this point it should be noted that dimer formation of DPH in the interphase can not be excluded as a possible reason for the observed red shift of the excitation spectra. However, the increase in both fluorescence life-times and fluorescence anisotropy decay times (see below) upon sorption of DPH in the alkyl phase leads us to assume that the extent of dimer formation is negligible. This assumption is supported by investigations of DPH bound covalently to polystyrene microbeads via polyethyleneglycol spacers at local concentrations very similar to those in the present alkyl phases. In the microbeads, aggregation of DPH occurred when no solvent was present, but vanished upon addition of solvent, e.g., acetonitrile. Whereas the polarizability in C_6 is not much different from that of the mobile phase, the polarizability of the C_{30} phase exceeds that of bulk decane significantly. Several effects contribute to the increase in polarizability with growing alkyl chain length. The density of highly polarizable organic material on the silica surface increases. As a result of the growing thickness of the bonded phase, the distance of sorbed probe molecules from both the silica surface and the mobile phase increases. As shown below, with increasing alkyl chain length, also lesser amounts of the highly polar solvent are sorbed in the interphase, thus further increasing the concentration of highly polarizable organic material in the immediate proximity of the probe molecules.

The molar fractions, x_{stat}, of DPH sorbed in the interphase are calculated from the areas under the stationary and mobile components of the fluorescence decay traces, $A_{stat} \cdot \tau_{F,stat}$ and $A_{mob} \cdot \tau_{F,mob}$ and the respective fluorescence quantum yields,

$\Phi_{F,stat}$ and $\Phi_{F,mob}$

$$x_{stat} = \frac{A_{stat} \cdot \tau_{F,stat} \cdot \Phi_{F,mob}}{A_{mob} \cdot \tau_{F,mob} \cdot \Phi_{F,stat}} \tag{6}$$
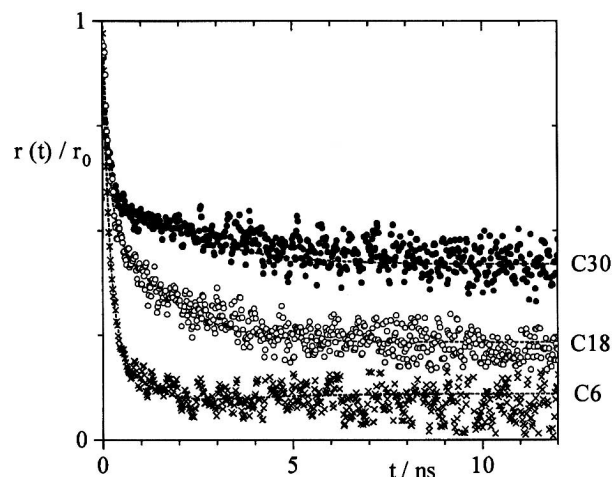
Fig. 4. Fluorescence anisotropy decay traces of DPH in suspensions of C_6, C_{18}, and C_{30} phases in acetonitrile/water mixtures (1:2, v/v). Points represent experimental data; dashed lines are the corresponding fits to Eq. (5).

Table III. Rotation Correlation Times, τ_R, Residual Anisotropies, r_∞, and Half-Cone Angles, θ, of DPH in Suspensions of C_6, C_{18}, and C_{30} HPLC Phases in Acetonitrile/Water Mixtures as Obtained from the Analysis of the Fluorescence Anisotropy Decay Traces According to Eq. (5)

Phase	τ_R (ns)	r_∞	θ (deg)
C_6			
Stationary	0.75	0.035	63
Mobile	0.18		
C_{18}			
Stationary	1.20	0.065	53
Mobile	0.18		
C_{30}			
Stationary	1.50	0.13	42
Mobile	0.18		

As the quantum yields are not exactly known for sorbed DPH, an approximate value of $\Phi_F = 0.26$, corresponding to the value in ethanol is inserted. The results collected in Table II and illustrated in Fig. 3 show that the fraction of DPH partitioning into the alkyl phase increases with increasing chain length of the bonded phase, which is in agreement with the enhanced lipophilic character of the interphase with increasing alkyl chain length as evidenced by the polarizability data given above and the concomitantly growing volume of the interphase.[5,21,22]

The time-resolved fluorescence anisotropy decay traces of DPH in three HPLC phases (Fig. 4) show contributions from two major components. These components are again assigned to DPH in the mobile and in

the stationary phase. Fits of the traces to Eq. (5), inserting the fluorescence lifetimes and amplitudes of the two species obtained from the analysis of the fluorescence decay curves (Table II), render the rotation correlation times given in Table III and Fig. 3.

For DPH in the mobile phase the fluorescence anisotropy decays exponentially, with a rotation correlation time of $\tau_R = 0.18$ ns. No residual anisotropy for $t \to \infty$ is observed, as expected for molecules with unrestricted rotational mobility. DPH sorbed in the alkyl phase shows correlation times $\tau_R > 1$ ns, indicating increased microviscosity inside the bonded phase. Concomitantly, residual anisotropies for infinitely long times are observed, which means that not all degrees of freedom are available for the rotational motion of the probe molecule in the interphase. In terms of the "wobble-in-cone" model,[23] the motion is restricted to a cone, whose angle can be calculated from the residual anisotropy according to Eq. (4). Obviously DPH, due to its nonpolar nature, is forced in between the bonded alkyl chains by the extremely polar solvent, even in the case of the shortest bonded phase, C_6. Owing to its rod-like shape, DPH is able to enter the interphase even if the alkyl chains are not fully extended, as is probably the case under the conditions used in our experiments. Both correlation time and residual anisotropy rise with increasing bonded phase chain length (Fig. 3). This is evidence that the microviscosity inside the alkyl phase increases and the cone angle decreases with growing chain length (Table III).

Solid-state NMR spectroscopy provides information about the order and mobility of the bonded alkyl chains themselves and thus helps us to understand the chain-length dependence of the microenvironment and of the mobility of DPH in the alkyl bonded phases. Figure 5 shows the methylene group signal in the ^{1}H-MAS NMR spectra of C_{18} and C_{30} chromatographic phases. Increasing line width indicates decreasing mobility with growing chain length. Concomitantly, the contribution of trans conformations increases with growing chain length, thus indicating enhanced order of the alkyl chains. This conclusion is drawn from the different ratios of the trans and gauche peaks of the $(CH_2)_n$ main chain signal at 32.6 and 30.0 ppm, respectively, in the ^{13}C CP/MAS NMR spectra of C_{18} and C_{30} phases (Fig. 6).

CONCLUSION

As revealed by solid-state NMR spectroscopy, the alkyl chains of bonded phases become less mobile and more extended with increasing ligand chain length, due
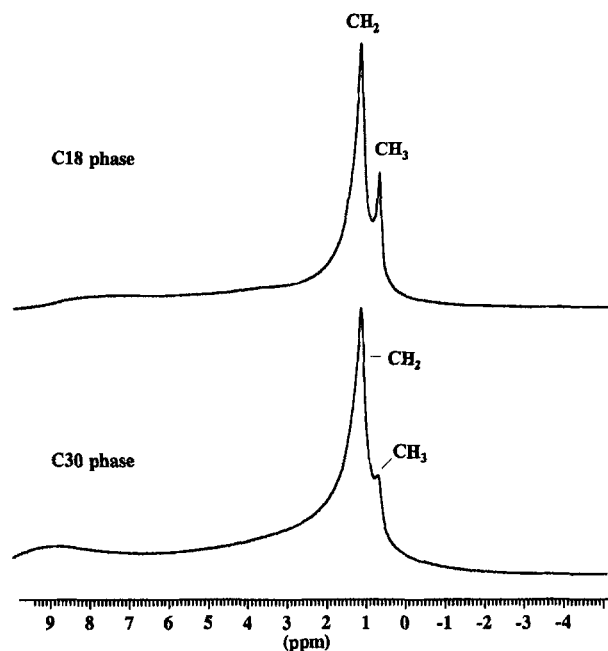
Fig. 5. ¹H MAS NMR spectra of dry C_{18} and C_{30} phases, showing the peak corresponding to the $(CH_2)_n$ groups.
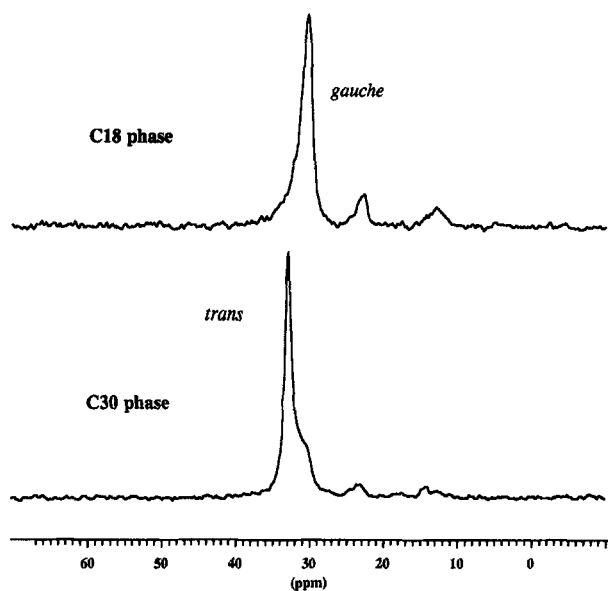

Fig. 6. ¹³C CP/MAS NMR spectra of dry C_{18} and C_{30} phases, showing the $(CH_2)_n$ peaks at $\delta = 30.0$ ppm and $\delta = 32.6$ ppm corresponding to the gauche and trans conformations of the alkyl chains, respectively.

to increasing van der Waals interactions between the chains. Thereby the number and size of interstices in the bonded phase are reduced for longer chains. Thus shape selectivity in HPLC separations is enhanced in favor of

rod-shaped molecules which are able to penetrate between the highly ordered chains. Concomitantly, the mobility of those solute molecules within the bonded phase is increasingly restricted with growing chain length, as evidenced by fluorescence anisotropy data. The spectral red shift of the fluorescence excitation spectra of DPH is indicative of greater polarizability in phases with longer ligand chains, which is due to the higher carbon density and the smaller fraction of sorbed solvent.

ACKNOWLEDGMENTS

REFERENCES

1. C. H. Lochmüller and D. R. Wilder (1979) *J. Chromatogr. Sci.* **17**, 574.
2. A. Tchapla, H. Colin, and G. Guiochon (1984) *Anal. Chem.* **56**, 621.
3. P. E. Antle and L. R. Snyder (1984) *LC Mag.* **2**, 840.
4. W. R. Melander and C. Horvath (1982) *Chromatographia* **15**, 86.
5. L. C. Sander and S. A. Wise (1987) *Anal. Chem.* **59**, 2309.
6. K. Albert, B. Pfleiderer, and E. Bayer (1990) in D. E. Leyden and W. T. Collins (Eds.), *Chemically Modified Surfaces, Vol. 3*, Gordon and Breach Science, New York, p. 233.
7. M. Pursch, R. Brindle, A. Ellwanger, L. C. Sander, C. B. Bell, H. Händel, and K. Albert (1997) *Solid State NMR* **9**, 191.
8. A. L. Wong, M. L. Hunnicutt, and J. M. Harris (1991) *Anal. Chem.* **63**, 1076.
9. J. Stahlberg, M. Almgren, and J. Alsins (1988) *Anal. Chem.* **60**, 2487.
10. V. M. Rangnekar, J. T. Foley and P. B. Oldham (1992) *Appl. Spectrosc.* **46**, 827.
11. M. E. Montgomery and M. J. Wirth (1992) *Anal. Chem.* **64**, 2566.
12. K. C. Hartner, J. W. Carr, and J. M. Harris (1989) *Appl. Spectrosc.* **43**, 81.
13. C. R. Mateo, M. P. Lillo, J. C. Brochon, M. Martinez-Ripoll, J. Sanz-Aparicio, and A. U. Acuna (1993) *J. Phys. Chem.* **97**, 3486.
14. M. Pursch, L. C. Sander, and K. Albert (1996) *Anal. Chem.* **68**, 4107.
15. M. Pursch, S. Strohschein, H. Händel, and K. Albert (1996) *Anal. Chem.* **68**, 386.
16. J. R. Lakowicz (1983) *Principles of Fluorescence Spectroscopy*, Plenum Press, New York.
17. S. L. Bondarev and S. M. Bachilo (1991) *J. Photochem. Photobiol.* **59**, 273.
18. C. H. Lochmüller, D. B. Marshall, and D. R. Wilder (1981) *Anal. Chim. Acta* **130**, 31.
19. J. W. Carr and J. M. Harris (1987) *Anal. Chem.* **59**, 2546.
20. B. Lehr, H.-J. Egelhaaf, H. Fritz, W. Rapp, E. Bayer, and D. Oelkrug (1996) *Macromolecules* **29**, 7931.
21. L. C. Sander and S. A. Wise (1993), *J. Chromatogr.* **656**, 335.
22. J. G. Dorsey and K. A. Dill (1989) *Chem. Rev.* **89**, 331.
23. M. van Gurp and Y. K. Levine (1989) *J. Chem. Phys.* **90**, 4095.